The Journal of Chemical Physics ARTICLE scitation.org/journal/jcp

Formation and detection of metastable formic acid in a supersonic expansion: High resolution infrared spectroscopy of the jet-cooled *cis*-HCOOH conformer

Cite as: J. Chem. Phys. 156, 204309 (2022); doi: 10.1063/5.0093401
Submitted: 28 March 2022 • Accepted: 2 May 2022 •
Published Online: 25 May 2022

Kirstin D. Doney,[1,2] Andrew Kortyna,[1,3] Ya-Chu Chan,[1,2] and David J. Nesbitt[1,2,4,a)]

AFFILIATIONS

[1] JILA, University of Colorado Boulder and National Institute of Standards and Technology, Boulder, Colorado 80309, USA
[2] Department of Chemistry, University of Colorado Boulder, Boulder, Colorado 80309, USA
[3] ColdQuanta, 3030 Sterling Circle, Boulder, Colorado 80301, USA
[4] Department of Physics, University of Colorado Boulder, Boulder, Colorado 80309, USA

[a)] **Author to whom correspondence should be addressed:** djn@jila.colorado.edu

ABSTRACT

High-resolution direct absorption infrared spectra of metastable *cis*-formic acid (HCOOH) trapped in a cis-well resonance behind a 15 kcal/mol barrier are reported for the first time, with the energetically unstable conformer produced in a supersonic slit plasma expansion of *trans*-formic acid/H_2 mixtures. We present a detailed high-resolution rovibrational analysis for *cis*-formic acid species in the OH stretch (ν_1) fundamental, providing first precision vibrational band origin, rotational constants, and term values, which in conjunction with *ab initio* calculations at the couple-cluster with single, double, and perturbative triple [CCSD(T)]/ANOn (n = 0, 1, 2) level support the experimental assignments and establish critical points on the potential energy surface for internal rotor trans-to-cis isomerization. Relative intensities for a- and b-type transitions observed in the spectra permit the transition dipole moment components to be determined in the body fixed frame and prove to be in good agreement with *ab initio* CCSD(T) theoretical estimates but in poor agreement with simple bond-dipole predictions. The observed signal dependence on H_2 in the discharge suggests the presence of a novel H atom radical chemical mechanism for strongly endothermic "up-hill" internal rotor isomerization between *trans*- and *cis*-formic acid conformers.

Published by AIP Publishing. https://doi.org/10.1063/5.0093401

I. INTRODUCTION

As the smallest carboxylic acid, formic acid (HCOOH) has been of fundamental interest for theoretical studies (see the work of Meyer and Suhm[1] and references therein), as well as an experimentally important molecule in combustion, atmospheric, and interstellar chemistry.[2–4] Of particular dynamical interest, HCOOH exists as both a stable and metastable excited isomer, which can, in principle, undergo unimolecular isomerization by internal rotation of the OH group around the C–O bond. This results in a ground vibrational state *trans*-HCOOH and the metastable excited state *cis*-HCOOH species, both with planar C_s symmetry as illustrated in Fig. 1. The more stable *trans*-HCOOH species is about 1365 cm^{-1} (3.9 kcal/mol) lower in energy relative to the cis-isomer, with a barrier[5] to internal rotation of about 4827 cm^{-1} (≈14 kcal/mol). As a result of this high barrier, the cis-isomer has been challenging to generate experimentally and has thus received far less attention than the well-studied ground state *trans*-formic acid species, including perturbation analysis.[6–10] Viewed from this perspective, the metastable *cis*-HCOOH conformer can, therefore, arguably be thought of as an "excited vibrational state" of the *trans*-HCOOH isomer, simply with requisite additional energy deposited into the internal rotor coordinate and resulting in extremely large angular shifts in the quantum probability.

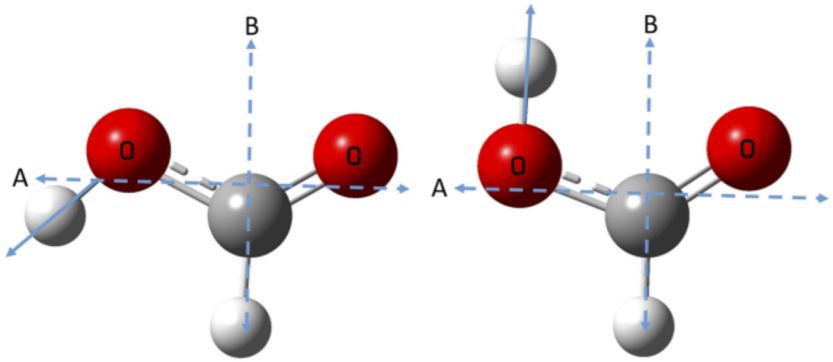

FIG. 1. The CCSD(T)/ANO2 equilibrium structures of (a) *cis*-HCOOH and (b) *trans*-HCOOH. Note that the OH bond in *cis*-formic acid lies $\theta \approx 43°$ from the A axis, predicting nearly equal A:B type band intensities in the simplest bond dipole model description.

The possibility of internal rotation between trans- and cis-isomers and the relative abundances of these two species is of particular dynamical interest in astrochemistry. For example, H atom abstraction from either of the two formic acid conformers might offer a possible novel non-equilibrium mechanism for the formation of *cis*- or *trans*-HOCO in interstellar ices.[4] The stable *trans*-HCOOH conformer was first detected in the interstellar medium (ISM) in 1971[11] and has since been observed in hot cores, hot corinos, dark clouds, and cometary coma by means of microwave[12–14] and infrared vibrational spectroscopy[15,16] and even through direct chemical analysis of chondritic meteorites.[17] Experimental microwave spectroscopy studies of both the *trans*- and metastable *cis*-HCOOH isomers by Winnewisser *et al.*[18] have enabled the first interstellar detection of the higher lying *cis*-HCOOH species in the Orion Bar photodissociation region (PDR).[19] Indeed, the detection of appreciable *cis*-HCOOH with a highly non-equilibrium cis-to-trans abundance ratio of 2.8 ± 1.0 suggested a novel mechanism for cis-to-trans "photo-switching" on icy grains due to abundant ultraviolet (UV) radiation and dynamics on electronically excited potential surfaces.[19] Such observations further highlight the value of additional microwave searches for interstellar formic acid, in particular the acquisition of more dynamical and spectroscopic information on the elusive metastable cis-isomer.[19] On a more terrestrial level, the presence of low lying isomers or rotamers in a combustion process can also result in anomalous temperature dependent heat capacities due to non-harmonic oscillator behavior yielding spurious vibrational state densities, which in turn can lead to distortions in kinetic modeling predictions based on statistical Rice–Ramsperger–Kassel–Marcus (RRKM) calculations.

In service to both these combustion and astrochemical goals, we initiated a successful high-resolution spectroscopic search in the mid-infrared for the *cis*-HCOOH conformer under slit jet discharge conditions. In what follows, we present first fully rotationally resolved rovibrational spectra for supersonically cooled *cis*-HCOOH in the OH stretch region near 3 μm. This paper is organized as follows: in Sec. II, we briefly describe the experimental approach, with the spectroscopic results and detailed rovibrational analyses presented in Sec. III. These results indicate excellent agreement with microwave spectroscopy by Winnewisser *et al.*[18] for the lower vibrational state of *cis*-formic acid, provide first high-resolution spectroscopic information on the $\nu_{OH} = 1$ OH stretch (ν_1) rovibrational manifold, and enable comparison with couple-cluster with single, double, and perturbative triple [CCSD(T)]/ANOn (n = 0, 1, 2) *ab initio* predictions. In Sec. IV, we present a Boltzmann analysis of spectral intensities to characterize the rotational temperature of the expansion, as well as the a-type to b-type band intensity ratios in order to extract transition dipole moment directions and make a direct comparison with high level *ab initio* calculations. Although the majority of the observed transitions are in excellent agreement with asymmetric top fits to a Watson Hamiltonian, we also find clear evidence for isolated rotational avoided crossings in $K_a = 1$ and 2 manifolds associated with the upper vibrational state, which are consistent with the predicted density of states at these internal energies and suggest the earliest stages of intramolecular vibrational coupling behavior. Finally, the novel nature of our "synthesis" and enhancement of metastable *cis*-formic acid signals by the addition of H_2 into the slit discharge allows us to speculate about dynamical formation pathways, with directions for further efforts and concluding remarks summarized in Sec. V.

II. EXPERIMENTAL METHOD

A description of the experimental setup has been presented previously in detail in the work of Davis *et al.*[20] For the current experimental configuration, the non-native isomer of formic acid (*cis*-HCOOH) is generated in a supersonically expanding pulsed planar plasma using Ar bubbled through temperature controlled formic acid liquid and subsequently combined with H_2 to obtain a variable mole fraction gas mixture of roughly $X_{Ar}/X_{H_2} \approx 4{:}1$ and $X_{HCOOH} \approx 3\%$. The resulting gas is then expanded into the vacuum chamber through a slit discharge nozzle with a negative polarity high voltage square wave (−650 V) applied to a pair of stainless steel jaws and modulated at 50 kHz over the ≈1000 μs duration of the gas pulse. The jaws are separated from the grounded valve body by a 1 mm Vespel insulator to form a 300 μm × 40 mm × 1 mm rectangular slit region through which the discharge current and the supersonically expanding gases counter propagate. As a result of typical gas flow velocities of 10^5 cm/s in an Ar/H_2 mixture, the formic acid spends only ≈1 μs in the discharge region, after which it cools rapidly (5–10 μs) over a 5–10 mm length scale in the subsequent 1D supersonic slit expansion.

To detect the *cis*-HCOOH molecules in this expansion, a frequency stabilized single mode ring dye laser (Spectra-Physics 380A,

R6G dye) is subtracted from a single mode Ar^+ laser (Spectra-Physics Series 2000, 515 nm) in a temperature-controlled periodically poled $MgO:LiNbO_3$ crystal (PPLN) to generate the required narrow-band continuous wave (cw) IR light source (5–10 μW, tunable from 2600 to 4600 cm^{-1}) via difference frequency generation. The IR laser light is then split using a dichroic mirror into signal (which is focused into a 16-pass Herriott cell inside the vacuum chamber) and reference beams. Due to spontaneous collisional collimation of longitudinal velocities in the 1D slit jet expansion, Doppler broadening along the slit axis direction is reduced by 10–20-fold, resulting in Doppler widths typically limited simply by the angular spread of the IR laser beams in the Herriot cell multipass.[21]

High-resolution IR spectra of the plasma products are then measured using phase-sensitive direct infrared laser absorption methods. The IR signal beam is multipassed with Herriott cell optics and intersects the expansion roughly ≈1 cm downstream from the nozzle body resulting in an absorbance path length of about 64 cm. To achieve near quantum shot noise limited absorption sensitivity, both the signal and reference beams are focused into balanced liquid-N_2 cooled InSb detectors with their outputs electronically subtracted in a fast, home-built balancing circuit and monitored via phase sensitive lock-in detection at the 50 kHz discharge modulation frequency. Relative frequency measurements with <10 MHz (<0.0003 cm^{-1}) precision during each 1–2 cm^{-1} scan segment are provided by interpolation of dye laser fringes transmitted through a Fabry–Pérot cavity, which is in turn locked to a polarization stabilized HeNe laser.[22] Absolute frequencies for a scan are obtained by calibration against CH stretch rovibrational transitions generated from CH_4 doped into the slit jet expansion, resulting in typical frequency precision and accuracy on the order of 12 MHz (0.0004 cm^{-1}).

III. RESULTS AND ANALYSIS

A. Initial spectral assignment to metastable *cis*-formic acid conformer

The path by which we stumbled on spectrally detecting the metastable *cis*-formic acid conformer warrants a brief description. We had previously performed multiple high-resolution studies spectroscopically characterizing the atmospherically important *trans*-HOCO radical and its H/D substituted *trans*-DOCO isotopomer at high (30:1) signal to noise.[20,23,24] What we had completely failed to detect, however, was the corresponding *cis*-HOCO radical species. Qualitatively similar to isomerization dynamics in *cis*/*trans*-HCOOH, this metastable *cis*-HOCO conformer lies behind an internal rotation torsion barrier, is slightly energetically uphill from the *trans*-HOCO radical, and yet proves to be a crucial radical intermediate along the complete oxidation pathway to H + OCO. Our logic was simply that the natural thermodynamic preference for *trans*-formic acid would pre-stabilize a cis-orientation of the OH and CO bonds, which upon cleavage of the CH bond would, therefore, preferentially form the desired *cis*-HOCO radical conformer. Our original strategy was that cleavage of the CH bond would be selectively achieved upon addition of H_2 to the stagnation gas mixture, specifically by chemical abstraction with H atom radicals formed copiously in the discharge. In agreement with expectations, we saw a set of strong OH stretch bands grow in the 3628–3646 cm^{-1} spectral region, significantly blue shifted from the OH stretch bands of *trans*-HOCO (near 3550 cm^{-1}) and indeed exhibiting 10–20× growth [from signal to noise (S/N) < 1 to S/N > 10] upon addition of H_2 to the discharge expansion mixture. Although our "synthesis" strategy proved flawed with respect to the clean generation of *cis*-HOCO, by way of compensation, this choice proved quite fortunate for the formation and detection of the novel metastable *cis*-formic acid conformer (*vide infra*).

At high resolution, the OH stretch gas phase spectrum of the more stable *trans*-HCOOH isomer near 3550 cm^{-1} is also readily observed; however, for this study, we focus only on this rich spectrum of additional lines between 3628 and 3646 cm^{-1}, displayed in a wide scan format in Fig. 2. Our initial assignment of this new band to the $v_{OH} = 1 \leftarrow 0$ stretch of the *metastable cis*-formic acid conformer relies on multiple experimental and theoretical observations. First, in Fig. 2, the 3636 cm^{-1} spectral band in the slit discharge expansion is composed of a uniform progression of tightly spaced $\Delta K_a = 0$ clusters, consistent with a strongly near prolate asymmetric top molecule with different moments of inertia ($I_a \ll I_b \approx I_c$). From body fixed directions of the OH group in each of the two conformers (see Fig. 1), the $v_{OH} = 1 \leftarrow 0$ stretch rovibrational band would be expected to be predominantly a-type (ΔK_a = even, ΔK_c = odd) or b-type (ΔK_a = odd, ΔK_c = odd) for the *cis*-and *trans*-formic acid species, respectively. The visual predominance of ΔK_a = even (a-type) transitions in Fig. 2, therefore, immediately identifies *trans*-formic acid as the very unlikely spectral carrier. Second, this OH band is significantly blue shifted (+86 cm^{-1}) from the OH spectral band of the *trans*-HCOOH conformer, which would be

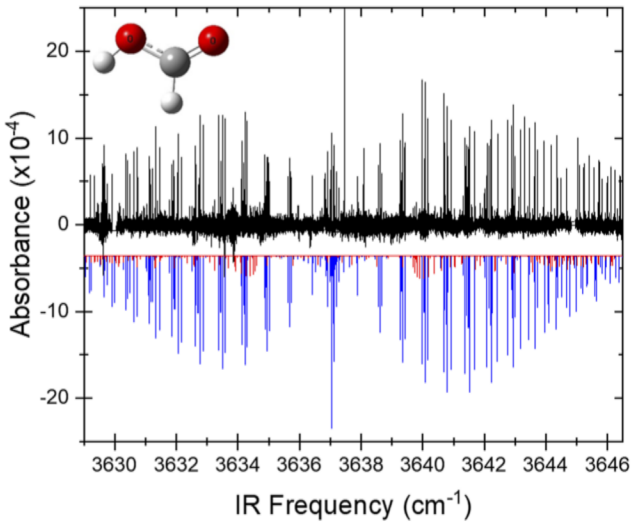

FIG. 2. The OH fundamental stretch spectrum (upward, black) of *cis*-formic acid formed from *trans*-formic acid in a H_2 slit supersonic discharge source, with a simulation (downward, red/blue) based on PGOPHER least squares fits to the data. The band structure is predominantly an a-type (blue) asymmetric top vibrational band, with approximately tenfold weaker contributions from b-type (red) intensity[15] plotted as well to help identify the assigned transitions. Note the slight dip in the overall intensity pattern in both P/R branch transition multiplets accessing the $J' = 6$ and 7 excited states, which arises from a local Coriolis interaction of the OH stretch with at least two near resonant dark states (see the supplementary material for details).

TABLE I. Spectroscopic parameters[a] (in cm^{-1}) from least squares fits to a OH stretching asymmetric top Hamiltonian model for *cis*-HCOOH.

	Ground[b]	ν_1
ν_0		3637.157 1(3)
A	2.884 05	2.873 3(3)
B	0.389 91	0.390 48(5)
C	0.343 04	0.342 16(5)
$\Delta_K \times 10^5$	7.88	33(1)
$\Delta_{JK} \times 10^6$	−2.38	6(2)
$\Delta_J \times 10^7$	2.79	9(2)
$\delta_K \times 10^6$	1.36	1.21(8)
$\delta_J \times 10^7$	0.473	−19(2)

[a]Experimental uncertainties are given in parentheses in units of the least significant digit.
[b]Fixed to ground state microwave values from Ref. 18.

consistent with a lack of intramolecular hydrogen bonding between the OH and carbonyl group in the *cis*- vs *trans*-HCOOH structure. The appearance of such a HCOOH band around 3637 cm^{-1} is, therefore, also too close to that of the *trans*-HCOOH isomer to be a combination band, yet too strong to be due to intensity sharing with multiple quanta vibrational states near resonant with OH stretch excitation in the *trans*-HCOOH isomer. Third, the 3637 cm^{-1} origin of this band is in excellent agreement with rotationally unresolved FTIR studies and spectral assignment to *cis*-formic acid by Meyer and Suhm in a heated (100–190 °C) nozzle expansion, though this information was in fact not available at the time of the initial measurements.[1] Despite the absence of rotational resolution in these earlier FTIR studies, their assignment of the spectral carrier as *cis*-formic acid in thermal equilibrium with *trans*-formic acid was confirmed by the strong enhancement of the cis/trans band intensity ratio at hot nozzle temperatures, as well as comparison with *ab initio* predictions. Of greatest dynamical interest in our own studies, however, the appearance of this OH stretch band reveals a strong (>tenfold) dependence on the presence or absence of H_2 coflowing in the discharge expansion gas mixture. This sensitivity to H_2, therefore, provides strong support for a novel production mechanism of the *cis*-formic acid carrier species mediated by H atom chemistry with the *trans*-formic acid conformer.

B. Confirmation of the *cis*-HCOOH assignment by rotationally resolved spectroscopy

Of course, high-resolution microwave/infrared spectroscopy itself offers powerful tools for unambiguous identification of the structure and atomic mass distributions for a given spectral carrier. Indeed, a complete high resolution analysis of the observed rovibrational band structure has been performed using the PGOPHER software,[25] based on a Watson non-rigid asymmetric top Hamiltonian model (A reduction and Ir representation). A zeroth order prediction of the infrared spectrum for *cis*-HCOOH is made simply based on lower state rotational constants (A_0, B_0, and C_0) previously determined from microwave studies,[18] yielding a characteristic near prolate asymmetric top a-type band pattern and in excellent agreement with the experimental observation (downward pointing peaks in Fig. 2). A preliminary round of assignments for the strong a-type ($\Delta K_a = 0$ and $\Delta K_c = \pm 1$) progressions is easily obtained, which in turn permits unambiguous identification of the spectral carrier to be *cis*-HCOOH by excellent agreement (<0.0002 cm^{-1}) with lower state combination differences predicted from the microwave constants.[18]

With the absorbing species confirmed to be the novel *cis*-HCOOH conformer, a more complete assignment of nearly all spectral features in the high-resolution spectrum is readily obtained. We fix the ground state constants to microwave values and then least squares fit the IR data to a Watson Hamiltonian in the A-reduction, floating upper state rovibrational plus quartic centrifugal distortion constants while freezing all higher order terms at the microwave ground state values (see Table I).[18] This choice is motivated by the use of A-reduction in the previous work, as well as that only quartic terms can be characterized with significance under low jet temperature conditions. In particular, the frequency results for $K_a = 0 \leftarrow 0$,

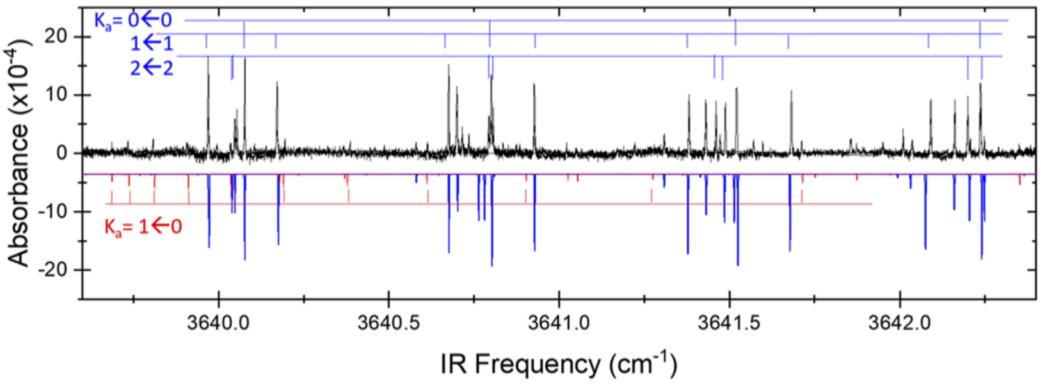

FIG. 3. A sample high resolution scan region [R(4)–R(7), black, upward] for the ν_1 OH stretch fundamental of *cis*-formic acid generated and cooled in a slit discharge supersonic expansion of *trans*-formic acid with H_2. For comparison, also shown are results of PGOPHER asymmetric top simulations (inverted, a-type/b-type bands in blue/red), based on the least squares fitted constants, an a-type/b-type intensity ratio of ≈10:1, and a rotational temperature of T_{rot} = 30 K. Discrepancies are noted particularly between predicted and observed line positions for transitions to $K'_a > 0$, which arise from weak Coriolis coupled rotational crossings between transitions accessing $J' = 7$–8 in the $K_a' = 1$ upper state manifold and transitions accessing $J' = 5$–6 in the $K_a' = 2$ in the upper state manifold (see the supplementary material for details).

3 ← 3, and 5 ← 5 a-type progressions are fit well, yielding a vibrational band origin at 3637.156(3) and residual standard deviation on the order of ±0.005 cm^{-1} (average deviation 0.0014 cm^{-1}). We note that although this quality of high-resolution spectroscopic fit is reasonable, it is still an order of magnitude larger than our frequency measurement uncertainties, signaling the presence of near-resonant state perturbations in the upper vibrational manifold. Indeed, even this modest quality of spectral fit to the Watson Hamiltonian does not extend successfully to the intermediate K_a' levels, with the $K_a = 1 \leftarrow 1$, K_c = J, and $K_a = 2 \leftarrow 2$ transitions exhibiting significantly larger spectral shifts in the fits (as much as 0.01 and 0.03 cm^{-1}, respectively; see Fig. 3). Given the highly local J-dependent nature of these shifts, we speculate that these arise from b-/c-type Coriolis interactions with at least two "dark" vibrational states of A″/A′ symmetry, respectively, in close accidental resonance with the $v_{OH} = 1$ manifold. As perturbation dynamics are not the main focus of this work, the analysis efforts to include such couplings in the Hamiltonian fit are deferred to the supplementary material, where they are more explicitly addressed. For the moment, it suffices to say that inclusion of two such Coriolis interacting states in a PGOPHER analysis yields greatly improved least squares fits with residual standard deviations more on the order of our experimental measurement uncertainties.

C. Comparison with *ab initio* calculations

We can further confirm our assignment and analysis of *cis*-HCOOH by comparison with high level *ab initio* CCSD(T) calculations, taking advantage of the CFOUR computational platform and Atomic Natural Orbital (ANOn, n = 0, 1, 2) basis sets developed by Almlöf and Taylor.[26] *Ab initio* calculations carried out at the couple-cluster with single, double, and perturbative triple [CCSD(T)] level of theory have been performed to determine estimates of the anharmonic vibrational energies and vibrationally dependent rotational constants of both *cis*- and *trans*-HCOOH to complete the sparse rovibrational information available; for all calculations, the development version of the CFOUR program is used.[27] Equilibrium geometry and second-order vibrational perturbation

TABLE II. CCSD(T)/ANO1 anharmonic (VPT2) frequencies and vibration–rotation interaction constants (in cm^{-1}) of HCOOH.[a]

Mode v_i	Obs. freq.	Vibrationally excited rotational constants (cm^{-1})		
		A_i	B_i	C_i
		cis-HCOOH ground		
	...	2.872 36 (*2.884 05*[b])	0.386 37 (*0.389 91*[b])	0.3401 2 (*0.343 04*)
v_1 O–H str.	3640.3 (*3637.1509*[c])	2.858 80 (*2.875 8*[c])	0.386 17 (*0.390 42*[c])	0.340 33 (*0.342 22*[c])
v_2 C–H str.	2869.5 (*2899*[d])	2.849 33	0.385 84	0.334 91
v_3 C=O str.	1822.1 (*1808*[d])	2.831 45	0.3821 4	0.340 84
v_4 C–H rock	1393.1 (*1396*[e])	2.828 55	0.392 18	0.329 75
v_5 COH bend	1249.3 (*1244*[e])	2.998 98	0.384 30	0.335 40
v_6 C–O str.	1097.5 (*1108*[d])	3.005 58	0.376 92	0.339 48
v_7 OCO scissor	653.9 (*661*[e])	3.265 29	0.389 13	0.339 51
v_8 C–H wag	1014.8	2.620 74	0.376 91	0.336 23
v_9 O–H oop wag	488.3 (*493.420 509*[f])	2.334 44	0.374 20	0.339 80
		trans-HCOOH ground		
	...	2.576 57 (*2.585 53*[b])	0.398 28 (*0.402 12*[b])	0.344 41 (*0.347 44*[b])
v_1 O–H str.	3574.3 (*3550.5*[e])	2.457 63	0.381 51	0.338 39
v_2 C–H str.	2931.1 (*2952.9*[e])	2.794 93	0.395 74	0.341 31
v_3 C=O str.	1781.6 (*1767.2*[e])	2.407 04	0.386 48	0.345 07
v_4 C–H rock	1386.2 (*1381.0*[e])	2.643 40	0.388 42	0.332 32
v_5 COH bend	1215.4 (*1215.8*[e])	2.654 36	0.396 38	0.337 69
v_6 C–O str.	1102.5 (*1103.4*[e])	2.539 08	0.404 65	0.344 45
v_7 OCO scissor	639.2 (*686.1656*[g])	2.556 61	0.397 48	0.343 55
v_8 C–H wag	1034.7 (*1037.4*[e])	2.539 31	0.394 11	0.340 71
v_9 O–H oop wag	622.7 (*640.7251*[g])	2.563 50	0.398 45	0.344 32

[a]Experimental values in italics.
[b]Reference 18.
[c]This work.
[d]Reference 1.
[e]Reference 2 (in solid Ar).
[f]Reference 10.
[g]Reference 6.

theory (VPT2) calculations with full cubic and the semidiagonal part of the quartic force fields were computed using the frozen-core atomic natural orbital (ANO) basis set with two common truncations: [4s3p2d1f] for non-hydrogen atoms and [4s2p1d] for hydrogen (hereafter known as ANO1) and [5s4p3d2f1g] (non-hydrogen atoms) and [4s3p2d1f] (hydrogen) (hereafter known as ANO2).[26,28–30] This ANO1 basis set has been shown to accurately predict anharmonic vibrational frequencies and vibrationally averaged rotational constants for many electronic ground state radical systems.[31,32] The results are summarized in Table II, for which rotational constants in the vibrationally excited states are estimated in first order from

$$\mathrm{Xv} = \mathrm{X}_0 - \sum_{i}^{3N-6} a_i^X v_i, \tag{1}$$

where for a given vibration, $X_v = A_v$, B_v, and C_v are rotational constants, α_i^X are vibration–rotation interaction constants, $v_i = 1$ is the vibrational quantum number for the fundamental excitation, and $X_0 = A_0$, B_0, and C_0 reflect the experimentally determined ground state values.

IV. DISCUSSION

A. Rotational Boltzmann analysis and direction of the transition dipole moment

The identification and assignment of the two band types in the *cis*-formic acid OH stretch spectrum permit a further investigation of the alignment of the transition dipole moment vector in the body fixed frame. To achieve this, we need the integrated band intensities for the a-type and b-type contributions to the spectrum. This can be readily obtained from a semilogarithmic Boltzmann plot of the lower state populations [Pop(J_{KaKc})], which are proportional to signal transition intensities scaled to Honl–London factor and lower state m_J degeneracy. As illustrated in Fig. 4, both a- and b-type bands follow a simple logarithmic relationship quite well, with a slope of $-1/kT_{rot}$ and an intercept reflecting (modulo a constant logarithmic offset) the integrated band intensity and square modulus of the transition dipole moment. Since the rotational distributions from which these two bands arise must be identical, the Boltzmann fits are constrained to the same slope, yielding a rotational temperature of T_{rot} = 29(3) K and a difference in logarithmic intercepts of 2.32(1). This rotational temperature is typical of the discharge slit jet expansion as verified for several other radical species,[20,23,24] with the temperatures slightly hotter due to the addition of H_2 to the expansion mixture.

Of greater quantitative physical interest is the difference in intercepts of 2.32(1), which translates into an a-type to b-type band intensity ratio of 10.2(1). In the dipole approximation, this ratio should be $\tan^2(\theta)$, where θ is the angle between the transition moment vector and body fixed A principal axis. The measured ratio of band intensities, therefore, yields an angle $\theta_{exp} = +17(1)^\circ$, in qualitative agreement with expectations of a transition moment largely aligned along the A inertial axis (see Fig. 1). This should be compared with *ab initio* calculations at the highest CCSD(T)/ANO2 level, which predict a slightly larger transition dipole moment angle of $\theta_{ab\ initio} = +22^\circ$. We do not yet know the origin of this modest difference, though the fit quality for the Boltzmann plot in Fig. 4 suggests it to be outside of our current experimental error.

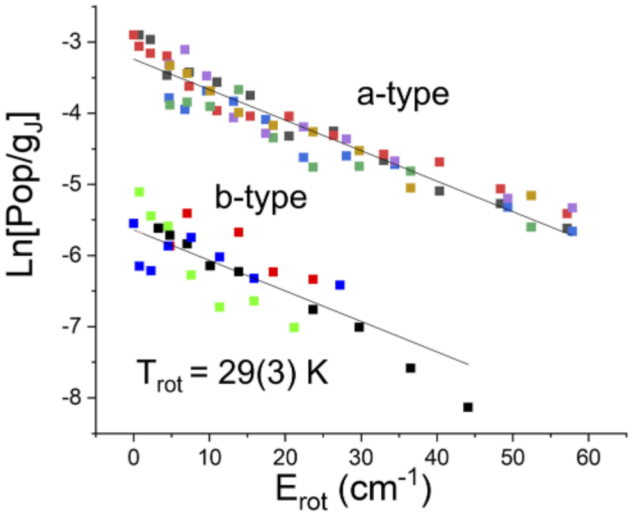

FIG. 4. A Boltzmann plot of the quantum state resolved populations vs internal rotational energy for *cis*-formic acid in the ground vibrational state, based on experimentally observed transitions in the $\nu_1 = 1 \leftarrow 0$ manifold. It is worth stressing that these a- and b-type transitions are plotted separately but reflect the same lower states with the same rotational temperature, which from their respective y-intercepts permits quantitative extraction of the experimental b-type to a-type band ratio [0.098(1)] for the ν_1 OH stretch. This ratio translates into a transition dipole moment angle with respect to the A axis of roughly $\theta \approx 17(1)^\circ$, which is in good qualitative agreement with CCSD(T)/ANO2 predictions ($\theta_{ab\ initio} = 22.9^\circ$). Interestingly, however, both experiment and theory differ dramatically from the geometric predictions [$\theta_{bond\text{-}dipole} \approx 44(1)^\circ$] from a simple bond dipole model. Such strong rotation of the dipole transition moment toward the A axis would be consistent with a resonance delocalization of negative charge between the two oxygen atoms in the vibrational limit of formate anion ($HCOO^-$) + H^+. See the text for more details.

More interestingly, however, both these experimental and theoretical predicted angles differ dramatically from expectations based on the simple bond dipole model [$\theta_{bond\ dipole} = +44(1)^\circ$], whereby the oscillator strength for the OH stretch is assumed to arise from the displacement of fixed charges on the O and H atoms. Such an overestimate of the transition moment angle signals a strong deviation from dipole bond model behavior, consistent with substantial vibrationally mediated electron flow away from the OH to the C=O carboxyl group upon extension of the OH bond. Strong rotation of the dipole transition moment toward the A axis is consistent with resonance delocalization of negative charge in formate anion ($HCOO^-$) in the vibrational limit of complete removal of the acidic proton.

B. A potential energy surface for internal rotation

The surprising but unambiguous presence of this metastable *cis*-formic acid in the slit discharge expansion source invites questions as to a more detailed formation mechanism. One first comment is that this *cis*-isomer geometry simply reflects a high lying local minimum on the same Born–Oppenheimer potential surface as the trans-isomer global minimum, i.e., *cis*-formic acid can be thought of as a "vibrationally excited state" of the *trans*-isomer species. To gain further insight into this unusual perspective, we have calculated a vibrationally adiabatic *ab initio* potential energy surface for

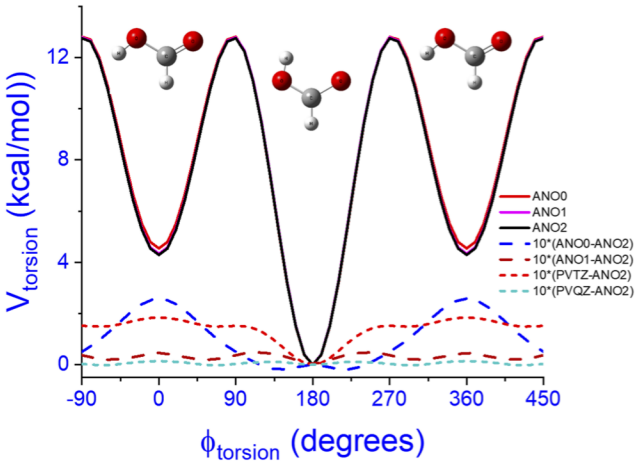

FIG. 5. Torsional potential (for 10° steps) for trans-to-cis isomerization in formic acid, calculated with CFOUR *ab initio* codes at the CCSD(T) level with the Amlof ANOn (n = 0, 1, 2) basis sets. All energies are referenced to zero at the *trans*-formic acid geometry ($\phi_{torsion}$ = 180°). Note the rapid convergence in the barrier height ($\Delta E_{barrier}$ = 12.75 kcal/mol) and energy differences (ΔE = 4.29 kcal/mol) between *trans*- and *cis*-isomers with basis set size. Also shown in dashed lines are deviations × 10 between results from Dunning/Pople PVnZ (n = 2, 3, 4) basis sets with the highest level ANO2 basis set, which serves to further illustrate the near equivalence of ANO1 and PVQZ basis sets and suggests convergence in energy differences at the <1 kcal/mol and even 0.1 kcal/mol level.

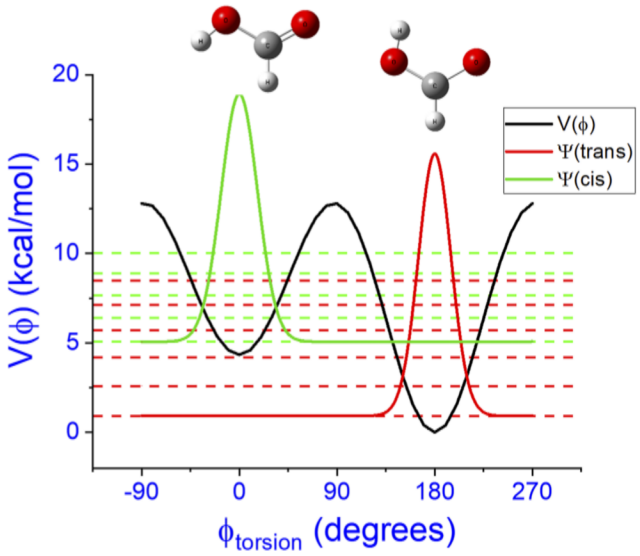

FIG. 6. Lowest 11 eigenvalues and select eigenfunctions for a vibrationally adiabatic treatment of the trans-to-cis isomerization, based on a CCSD(T)/ANO2 potential, a reduced moment of inertia I($\phi_{torsion}$) from LAMM/Multiwell calculations[33] and Numerov integration of the resulting 1D Schrödinger equation. Note that these irregular eigenvalue patterns can be deconstructed into two more nearly harmonic progressions corresponding to "local" torsional excitation of the trans (red) and cis (green) conformers of formic acid. This is further confirmed by analysis of the eigenfunctions, which are clearly localized in the trans well for the lowest few states but acquire strong cis conformer character starting at the third excited state. Alternatively stated, *cis*-formic acid is a vibrationally excited "resonance" state of the *trans*-formic acid conformer.

internal torsion of the COH group (5° grid spacing), relaxing all other degrees of internal freedom as a function of torsional angle. To ensure sufficient convergence of this potential surface, we have performed sequential *ab initio* calculations at the CCSD(T)/ANOn (n = 0, 1, 2) level, which allows us to monitor the dependence on basis set quality. The results of such calculations are summarized in Fig. 5 where all three adiabatic potential surfaces have been obliged to coincide at the ground state "*trans*-formic acid" geometry.

First, the results demonstrate a rapid convergence with basis set size, at a level that suggests isomerization barrier height and energy difference accuracies at the few 0.1 kcal/mol level. Particularly noteworthy are incremental changes in the ANOn–ANO2 results, which have been expanded by an additional tenfold in Fig. 5. Given the rapid convergence in these sequences, the relative energies of *cis*- and *trans*-isomers are predicted to be 4.29 kcal/mol, with a transition state trans-to-cis isomerization barrier of 12.75 kcal/mol. We have also performed these isomerization path calculations with Dunning correlation consistent PVnZ (n = 2, 3, 4) basis sets, which exhibit less rapid convergence but with CCSD(T)/PVQZ results in excellent (<0.1 kcal/mol) agreement with the highest level ANO2 basis set results. It is interesting to note that the residual errors in the PVTZ basis set results look to be comparable to values already obtained at the ANO0 level, and thus, for formic acid, the ANOn basis sets provide results comparable in accuracy to PV(n + 1)Z.

Second, in order to predict zero-point energies, eigenvalues, and eigenfunctions in this torsional isomerization pathway from an adiabatic 1D Schrödinger equation, we have used the LAMM utility in the MULTIWELL suite of codes to calculate the reduced moment of inertia from these adiabatically optimized geometries as a function of the internal rotor torsional coordinate.[33] Specifically, we calculate the reduced moment of inertia I(ϕ) in 10° steps from [0°, 180°] and use symmetry around the trans planar configuration and linear interpolation to extend over the full [0°, 360°] angular range. Treating this 1D torsional coordinate in the vibrationally adiabatic approximation, we then use Numerov's methods to solve the Schrödinger equation as a function of internal rotation angle to predict the lowest ten eigenvalues up to the isomerization barrier, as shown as the dashed horizontal lines in Fig. 6. Averaged over the full [0°, 360°] coordinate range, the nominal moment of inertia is I ≈ 0.42 amu Ang^2, which is consistent with the mostly torsional motion of the OH around the CO bond and counterrotation of the corresponding formyl group in the Eckert frame.

Of particular interest, the lowest three vibrational states are easily recognizable as a nominally harmonic vibrational progression of states (v_{trans} = 0, 1, 2) localized in the trans well (red dashed lines). However, the third excited state (green dashed line) breaks this near harmonic pattern and exhibits a nearly complete shift in quantum amplitude to the *cis*-formic acid conformer well. Furthermore, we can identify in the *cis*-formic acid wavefunction a new quasi-harmonic sequence of states (green dashed lines), which correspond to v_{cis} = 0, 1, 2, 3. . . excitation localized in the higher lying isomer well. In other words, the *cis*-formic acid conformer is nominally just a progression of strongly anharmonic excited states of *trans*-formic acid in the torsional coordinate. These two torsional wavefunction progressions in both cis and trans wells maintain their localized quasi vibrational nature until the rotational energies approach the isomerization barrier, at which point the wavefunctions begin to exhibit nodal behavior widely distributed over the

full range of torsional angles and more characteristic of a hindered internal rotor.

C. A putative H-atom reaction mechanism for "uphill" cis- to trans-isomerization

The one remaining question to be addressed is how the generation of this high lying metastable *cis*-formic acid conformer appears to be greatly enhanced in the slit jet discharge expansion. Due to ≈10 Torr level concentrations in the stagnation region, the corresponding OH stretch spectrum of *trans*-formic acid is unfortunately too saturated (i.e., optically black) to measure concentrations reliably. Furthermore, *trans*-formic acid can appear either by discharge modulated removal of lower states or formation of higher states, rendering phase sensitive detection less effective in quantitatively distinguishing these lines. Thus, we cannot yet quantify the relative populations of *cis*- vs *trans*-conformer species though we would strongly suspect it to be considerably non-equilibrium in any event. However, we can say that the OH stretch spectrum of the cis-isomer grows from undetectable (S/N < 1) to quite easily detectable (S/N > 20) with the introduction of only modest (several Torr level) partial pressures of H_2 into the discharge. Given that H_2 is readily dissociated in the discharge to form H atoms, it would seem plausible that the presence of abundant H atoms is responsible for formation of the metastable cis-isomer, a possibility we have explored with preliminary albeit high level *ab initio* calculations. Although validation will certainly require considerably more experimental studies combined with detailed *ab initio* and dynamics calculations, we can at least offer the following putative chemical mechanism for preferential formation of the cis-conformer in a H_2 discharge.

Specifically, the radical addition of a single H atom to the formic acid carbonyl group is energetically accessible to form the dihydroxymethyl radical, over a barrier that is significant but distinctly lower than that of cis-to-trans isomerization. Once in the highly energized dihydroxymethyl radical form, internal rotation of the two hydroxy groups can proceed rapidly over an energetically very much lower barrier (<1 kcal/mol). This permits the radical to achieve a highly energized geometry with both trans- and cis-orientations of the two OH groups, stabilized by internal hydrogen bonding in a dipole–dipole configuration. What makes this relevant is that the pair of O atoms in dihydroxymethyl are now equivalent. Thus, subsequent loss of the radical H atom from this highly energized intermediate could, in principle, occur from either of the OH groups, resulting in the formation of the corresponding *cis*- or *trans*-formic acid conformer and stabilized in their respective deep torsional wells. Of course, the overall ≈4 kcal/mol energy difference between the *cis*- and *trans*-formic acid isomers must come from somewhere, but this, in principle, could be easily provided via H atom abstraction from one of the two OH groups by secondary H atoms present in the discharge.

V. SUMMARY AND CONCLUSION

The high-resolution infrared spectra of *cis*-formic acid (*cis*-HCOOH) in the OH stretch vibrational region around 3600 cm^{-1} recorded in a supersonic planar plasma jet are presented. A detailed rotational analysis is performed, including deperturbation of two Coriolis interactions, resulting in spectroscopic parameters for the fundamental vibrational state and band origins for the perturbing states (see the supplementary material for more detailed analysis). Agreement with *ab initio* predictions is uniformly good. *Ab initio* predictions for the fundamental vibrational modes and associated vibrational dependent rotational constants for both *cis*- and *trans*-formic acid are presented to aid future experimental and astronomical searches. Finally, 1D vibrationally adiabatic potential energy surfaces along the torsional coordinate are calculated at CCSD(T)/ANOn (n = 0, 1, 2) levels. A reduced $B_{int}(\phi)$ constant for internal rotation is calculated from these *ab initio* relaxed geometries with the help of Multiwell and LAMM software,[33] which makes a feasible direct solution of the 1D Schrödinger equation in the torsional coordinate, yielding clear anharmonic progressions of vibrationally excited states localized in the cis and trans wells.

SUPPLEMENTARY MATERIAL

The IR spectra for *cis*-formic acid are perturbed by coupling between the "bright" state and near resonant "dark" states, which can be successfully characterized by including two separate Coriolis interactions in the upper $K_a' = 1$ and 2 manifolds. Details of this deperturbation analysis are presented in the supplementary material.

ACKNOWLEDGMENTS

This work was supported by grants from the Department of Energy (Grant No. DE-FG02-09ER16021), with initial funds for the construction of the slit-jet laser spectrometer provided by the National Science Foundation (Grant Nos. CHE-1665271 and PHY 1734006). K.D.D. would like to thank the NIST NRC Postdoctoral Research Associateship Program for financial support. We wish to also thank John Stanton and T. Lam Nguyen for their patient and gracious help in implementing the CFOUR and LAMM/Multiwell software packages, respectively.

AUTHOR DECLARATIONS

Conflict of Interest

The authors have no conflicts to disclose.

DATA AVAILABILITY

The data that support the findings of this study are available from the corresponding author upon reasonable request.

REFERENCES

[1] K. A. E. Meyer and M. A. Suhm, "Stretching of *cis*-formic acid: Warm-up and cool-down as molecular work-out," Chem. Sci. **10**, 6285 (2019).
[2] M. Pettersson, J. Lundell, L. Khriachtchev, and M. Räsänen, "IR spectrum of the other rotamer of formic acid, *cis*-HCOOH," J. Am. Chem. Soc. **119**, 11715 (1997).
[3] P. H. Wine, R. J. Astalos, and R. L. Mauldin, "Kinetic and mechanistic study of the hydroxyl + formic acid reaction," J. Phys. Chem. **89**, 2620 (1985).

[4]M. N. Markmeyer, T. Lamberts, J. Meisner, and J. Kästner, "HOCO formation in astrochemical environments by radical-induced H-abstraction from formic acid," Mon. Not. R. Astron. Soc. **482**, 293 (2019).
[5]W. H. Hocking, "Other rotamer of formic-acid, cis-HCOOH," Z. Naturforsch., A **31**, 1113 (1976).
[6]A. Perrin, J.-M. Flaud, B. Bakri *et al.*, "New high-resolution analysis of the ν_7 and ν_9 fundamental bands of *trans*-formic acid by Fourier transform infrared and millimeter-wave spectroscopy," J. Mol. Spectrosc. **216**, 203 (2002).
[7]H. Kuze, T. Amano, and T. Shimizu, "High-resolution laser spectroscopy of the ν_3 vibration-rotation band of HCOOH," J. Chem. Phys. **77**, 714 (1982).
[8]W. H. Weber, P. D. Maker, J. W. C. Johns, and E. Weinberger, "Sub-Doppler laser-Stark and high resolution Fourier transform spectroscopy of the ν_3 band of formic acid," J. Mol. Spectrosc. **121**, 243 (1987).
[9]J.-C. Deroche, J. Kauppinen, and E. Kyrö, "ν_7 and ν_9 bands of formic acid near 16 μm," J. Mol. Spectrosc. **78**, 379 (1979).
[10]O. I. Baskakov, V.-M. Horneman, J. Lohilahti, and S. Alanko, "High resolution FTIR spectra of the ν_9 vibrational band of *cis*-rotamers HCOOH and $H^{13}COOH$," J. Mol. Struct. **795**, 49 (2006).
[11]B. Zuckerman, J. A. Ball, and C. A. Gottlieb, "Microwave detection of interstellar formic acid," Astrophys. J. **163**, L41 (1971).
[12]J. Cernicharo, N. Marcelino, E. Roueff *et al.*, "Discovery of the methoxy radical, CH_3CO, toward B1: Dust grain and gas-phase chemistry in cold dark clouds," Astrophys. J. Lett. **759**, L43 (2012).
[13]S. Y. Liu, D. M. Mehringer, and L. E. Snyder, "Observations of formic acid in hot molecular cores," Astrophys. J. **552**, 654 (2001).
[14]S. Cazaux, A. G. G. M. Tielens, C. Ceccarelli *et al.*, "The hot core around the low-mass protostar IRAS 16293-2422: Scoundrels rule!," Astrophys. J. **593**, L51 (2003).
[15]D. Bockelee-Morvan, D. C. Lis, J. E. Wink *et al.*, "New molecules found in comet C/1995 O1 (Hale-Bopp)—Investigating the link between cometary and interstellar material," Astron. Astrophys. **353**, 1101 (2000).
[16]J. V. Keane, A. G. G. M. Tielens, A. C. A. Boogert, W. A. Schutte, and D. C. B. Whittet, "Ice absorption features in the 5–8 μm region toward embedded protostars," Astron. Astrophys. **376**, 254 (2001).
[17]J. F. Briscoe and C. B. Moore, "Determination of formic and acetic acid in chondritic meteorites," Meteoritics **28**, 330 (1993).
[18]M. Winnewisser, B. P. Winnewisser, M. Stein *et al.*, "Rotational spectra of *cis*-HCOOH, *trans*-HCOOH, and *trans*-$H^{13}COOH$," J. Mol. Spectrosc. **216**, 259 (2002).
[19]S. Cuadrado, J. R. Goicoechea, O. Roncero *et al.*, "*Trans-cis* molecular photoswitching in interstellar space," Astron. Astrophys. **596**, L1 (2016).
[20]S. Davis, M. Fárník, D. Uy, and D. J. Nesbitt, "Concentration modulation spectroscopy with a pulsed slit supersonic discharge expansion source," Chem. Phys. Lett. **344**, 23 (2001).
[21]C. M. Lovejoy and D. J. Nesbitt, "Slit pulsed valve for generation of long path-length supersonic expansions," Rev. Sci. Instrum. **58**, 807 (1987).
[22]E. Riedle, S. H. Ashworth, J. T. Farrell, and D. J. Nesbitt, "Stabilization and precise calibration of a continuous-wave difference frequency spectrometer by use of a simple transfer cavity," Rev. Sci. Instrum. **65**, 42 (1994).
[23]C.-H. Chang, G. T. Buckingham, and D. J. Nesbitt, "Sub-Doppler spectroscopy of the *trans*-HOCO radical in the OH stretching mode," J. Phys. Chem. A **117**, 13255 (2013).
[24]A. Kortyna and D. J. Nesbitt, "High-resolution infrared spectroscopy of jet cooled *trans*-deuteroxycarbonyl (*trans*-DOCO) radical," J. Chem. Phys. **150**, 194304 (2019).
[25]C. M. Western, "PGOPHER: A program for simulating rotational, vibrational and electronic spectra," J. Quant. Spectrosc. Radiat. Transfer **186**, 221 (2017).
[26]J. Almlöf and P. R. Taylor, "General contraction of Gaussian-basis sets. I. Atomic natural orbitals for first and second-row atoms," J. Chem. Phys. **86**, 4070 (1987).
[27]D. A. Matthews, L. Cheng, M. E. Harding *et al.*, "Coupled-cluster techniques for computational chemistry: The CFOUR program package," J. Chem. Phys. **152**, 214108 (2020).
[28]I. M. Mills, in *Molecular Spectroscopy: Modern Research*, edited by K. N. Rao, and C. W. Mathews (Academic, New York, 1972), Vol. 1, p. 115.
[29]D. Feller, "The role of databases in support of computational chemistry calculations," J. Comput. Chem. **17**, 1571 (1996).
[30]K. L. Schuchardt, B. T. Didier, T. Elsethagen *et al.*, "Basis set exchange: A community database for computational sciences," J. Chem. Inf. Model. **47**, 1045 (2007).
[31]J. Vázquez and J. F. Stanton, "Treatment of Fermi resonance effects on transition moments in vibrational perturbation theory," Mol. Phys. **105**, 101 (2007).
[32]K. D. Doney, D. Zhao, J. Bouwman, and H. Linnartz, "The high-resolution infrared spectrum of the $\nu_3 + \nu_5$ combination band of jet-cooled propyne," Chem. Phys. Lett. **684**, 351 (2017).
[33]J. R. Barker, T. L. Nguyen, J. F. Stanton *et al.*, Multiwell Program Suite, 2021.